Innovations in Gemini Adaptive Optics System Design

Glen Herriot, Simon Morris, Scott Roberts, Murray Fletcher, Leslie Saddlemyer, Gurjeet Singh,
Jean-Pierre Véran, E. H. Richardson
Herzberg Institute of Astrophysics, National Research Council of Canada
5071 W. Saanich Rd., Victoria BC, Canada V8X 4M6

ABSTRACT

The Gemini Adaptive Optics System, (Altair), under construction at the Dominion Astrophysical Observatory of the National Research Council of Canada's Herzberg Institute of Astrophysics is unique among AO systems. Altair is designed with its deformable mirror (DM) conjugate to high altitude. This concept is only practical at an observatory where extraordinary measures have been taken to reduce local (near ground level) seeing degradation. We summarize these measures. We then describe Altair.

Both the Wavefront sensor foreoptics and control system are unconventional, because the guide star footprint on an altitude-conjugated DM moves as the guide star position varies. During a typical nodding sequence, where the telescope moves 10 arcseconds between exposures, this footprint moves by half an actuator and/or WFS lenslet. The advantages of altitude conjugation include increased isoplanatic patch size, which improves sky coverage, and improved uniformity of the corrected field. Although the initial installation of Altair will use natural guide stars, it will include features to use a laser guide star (LGS) with minimal rework. Altitude conjugation also reduces focal anisoplanatism with laser beacons.

The infrastructure of Gemini observatory provides a variety of wavefront sensors and nested control loops that together permit some unique design concepts for Altair.

Keywords: Altair, Gemini, altitude, conjugate, adaptive, optics

SYSTEM DESCRIPTION

The Gemini adaptive optics system was recently renamed Altair, just prior to a successful preliminary design review in October 1997. We will have a critical design review in January 1999, and will commission Altair on the telescope in late 2000.

Altair is a large opto-mechanical and electronic instrument, 1.5 m x 1.5 m x 2.5 m, that will correct image distortion, caused by turbulent mixing of warm and cold air above Mauna Kea, Hawaii. Altair measures this distortion with a 12x12 SH wavefront sensor, and reflects the telescope light from a 177-actuator deformable mirror, bent to a new shape a thousand times per second. A Cassegrain-mounted facility of the telescope, Altair is designed to reproduce the original telescope beam exit pupil, f/ratio, and focal plane (with improved quality) and feed instruments operating in the visible and near infrared. Altair will deliver images with J band Strehl ratios of 0.4 in median seeing at zenith distances up to 45 degrees. This specification includes margin for distortions caused by the telescope and a typical instrument (i.e., Near-Infrared Imager). While the initial delivery of Altair will be a natural guide star system, it will allow convenient upgrades to use a laser beacon.

Altair mounts on a side face of the cube-shaped Instrument Support Structure (ISS). A fold mirror near the top of the ISS sends the light to Altair where it is processed and returned to a central fold mirror that directs the light to instruments on the other faces of the ISS.

As well as the name of a bright star in the Summer Triangle, Altair is an acronym for **ALT**itude conjugate **A**daptive optics for the **I**nfra**R**ed. Unique among adaptive optics projects, Altair's deformable mirror is at an image conjugate to the high altitude turbulent layer 6.5 km from the telescope. Analysis[5] by René Racine, Université de Montréal, shows that altitude conjugation typically will double the diameter of the corrected field. This will greatly increase the number of astronomical targets close enough to a guide star. However, it adds complexity to the optics, control system and wavefront sensor, and is less capable of correcting ground-level seeing than a traditional adaptive optics system with a deformable mirror conjugate to the telescope's primary mirror. This technical risk is only worth taking, because of Gemini's extraordinary measures, to reduce local seeing.

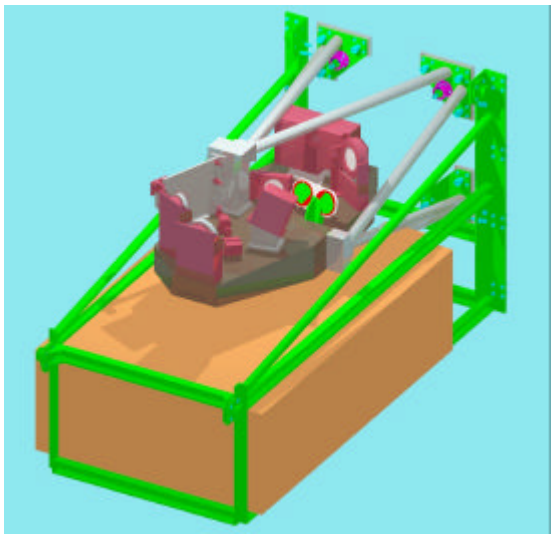

Figure 1 Altair

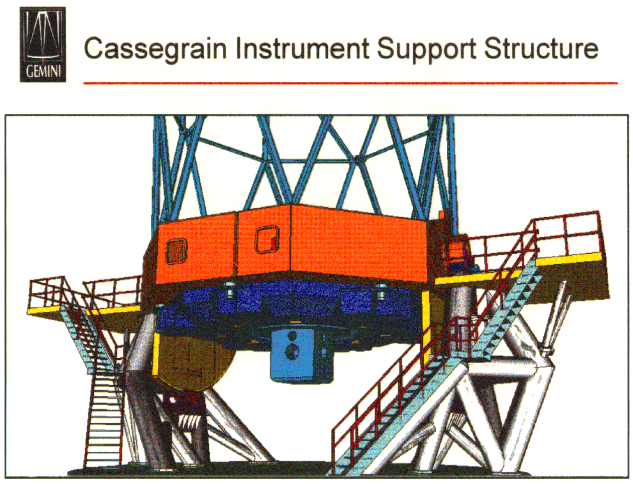

Figure 2 Gemini Telescope

LOCAL SEEING IMPROVEMENT

The Gemini Project has made tremendous effort to eliminate the effects of local seeing. Supercomputer and water tunnel modelling, of the wind flow over the summit and through the telescope dome, supported the following design features.

- High Pier, putting the primary mirror 20 m elevation, well above the 10 m thick boundary layer where prevailing winds mix with air warmed by the ground
- Huge exterior wind gates for passive dome flushing
- For observing during low wind-speed, active flushing fans draw air down through the telescope and observing floor to an exhaust tunnel
- Day time air conditioning and refrigeration of primary mirror
- Active fine control of primary mirror front-surface temperature by passing current through coating
- Refrigerated insulated enclosures for all electronics
- Cooling of motors, bearings and heat sources
- Low emissivity dome coating to prevent dome sub-cooling from creating a plume of cold air falling into slit
- Temperature control of secondary mirror positioning mechanism

WHY IS ALTAIR UNIQUE?

As well as the decision to altitude-conjugate the DM, several features of the Gemini observatory infrastructure led us to novel design ideas. Altair must feed standard Gemini Cassegrain-mounted instruments. Thus, it must reproduce the telescope beam under a varying gravity orientation. In return, each Gemini instrument has a 2x2 Shack-Hartmann WFS mounted as close as possible to the focal plane to sense tip/tilt and focus. These on-instrument WFS (OIWFS) greatly relieve the tolerance for thermal and gravity-induced flexure within Altair. As well, the ISS has a High Resolution 20x20 SH WFS useful for off-line calibration of the non-common path errors between the Altair WFS and the delivered image plane. Furthermore, Altair has the luxury of learning from past AO projects. Meanwhile, computer design has progressed to the point that a single modern RISC CPU reconstructor, re-optimized during an exposure, will control the deformable mirror. Taken together, these concepts have permitted some innovative engineering in Altair.

OPTICAL PACKAGING

In figure 3, you can see the beam from the telescope collimated and reflected from the deformable mirror and tip/tilt mirror before being transmitted through the beamsplitter. There is a changer mechanism to insert an optional L&M band beamsplit-

ter. Next, the science beam passes through a deployable atmospheric dispersion compensator, currently designed for 0.8 to 1.8 *m*m, although we are trying to extend it to 2.5 *m*m for cross-dispersed JHK spectroscopy. Because Altair is more than two metres upstream from an instrument focal plane, the diameter of the f/16 exit beam is larger than the deformable mirror. Therefore, a convex mirror expands the beam and a camera mirror reformats the output to imitate the raw telescope beam, while also flattening the focal plane.

The optics is mounted on an optical bench supported by a truss from the ISS[4]. The mass of Altair including electronics is 900 kg and its centre of gravity is 1200 mm from the mounting face, to maintain the balance of the telescope. The electronics, in an insulated and cooled enclosure below the optical bench, consume nearly 2 kW, but leak < 100 W into the dome.

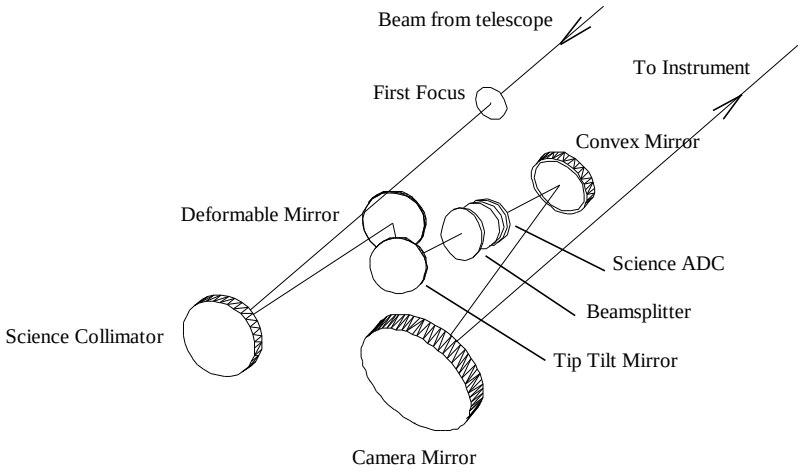

Figure 3 Science Optical Path

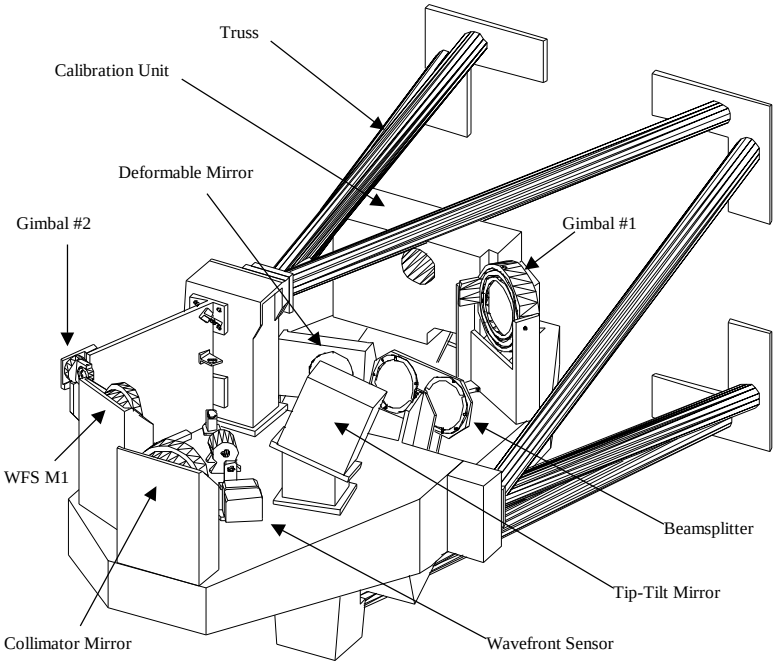

Figure 4 Opto-mechanical bench

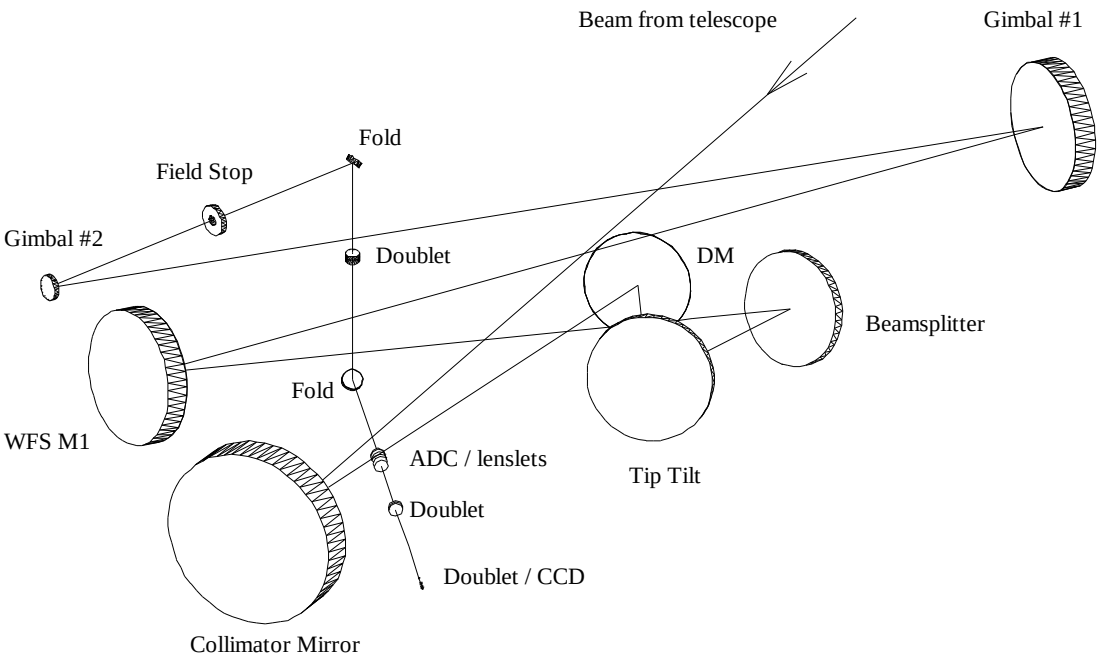

Figure 5 NGS WFS optical path

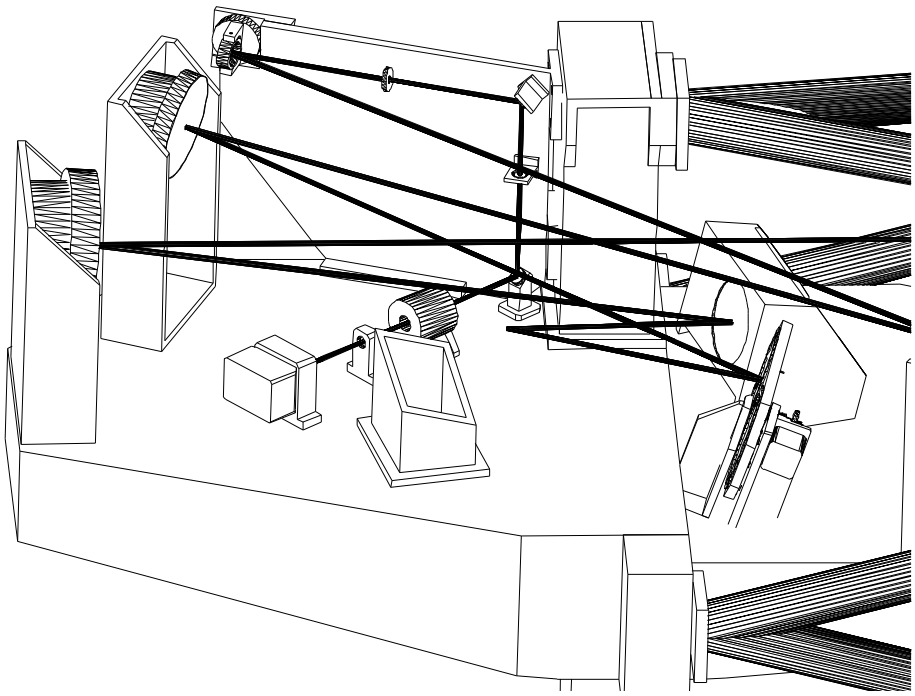

Figure 6 NGS AOWFS packaging

NATURAL GUIDE STAR WAVEFRONT SENSOR OPTICS.

As mentioned earlier, the beamsplitter reflects the WFS light. This remarkable beamsplitter, from Lumonics Optical in Ottawa, transmits >97% from 0.85 to 2.5 *m*m, and reflects >99% of visible light from 0.4 *m*m to 0.83 *m*m. This polarity of beamsplitter is more efficient at both transmission and reflection than a short-wave pass coating. Even though transmitting the science light causes a slight increase in emissivity, this is more than compensated by higher WFS throughput. The resulting higher Strehl ratio means that integration times for equivalent signal to noise ratio, are shorter by a factor of 2-4 with typical guide stars.

After the beamsplitter, a conic mirror refocuses the guide star. On the path to the focus, two flat gimballed mirrors fold the beam, select a guide star in the 2 arcminute field, and steer it through the field stop. Then the WFS light is collimated onto an ADC and lenslet array and then demagnified onto an EEV 39 CCD, which remains stationary on the optical bench. Each spot falls on a quad-cell of four pixels surrounded by two guard rows and columns that are skipped to save read time. In Figure 6, you can see the entire path from the beamsplitter changer to the CCD, with the tip/tilt mirror removed for clarity. While acquiring the guide star, the gimbal mirrors maintain alignment between the DM and the WFS. Each square region defined by four adjacent actuators is always imaged onto the same lenslet. To accommodate ±1 mm tolerance to the focal plane of various instruments, the AO WFS is refocused by 2 mm of axial travel on the second gimbal mirror.

LASER GUIDE STAR WFS OPTICS.

The current plan is to upgrade Altair to use a laser beacon. Thus we have included a concept for additional optics and a second WFS. The laser guide-star light follows the science path to the beamsplitter and then follows the natural guide star path including the two gimbal mirrors. These foreoptics can acquire laser guide stars throughout field of view 1 arcminute in diameter. Figure 7, Laser Guide Star Optics, begins with the reflection from the second gimbal mirror. A perforated mirror replaces the field stop at the natural guide star focus. Since a laser beacon is out of focus at the NGS focus, the laser light reflects from the mirror, while the natural starlight passes through a 1.2 arcsecond hole, smaller than the shadow of the

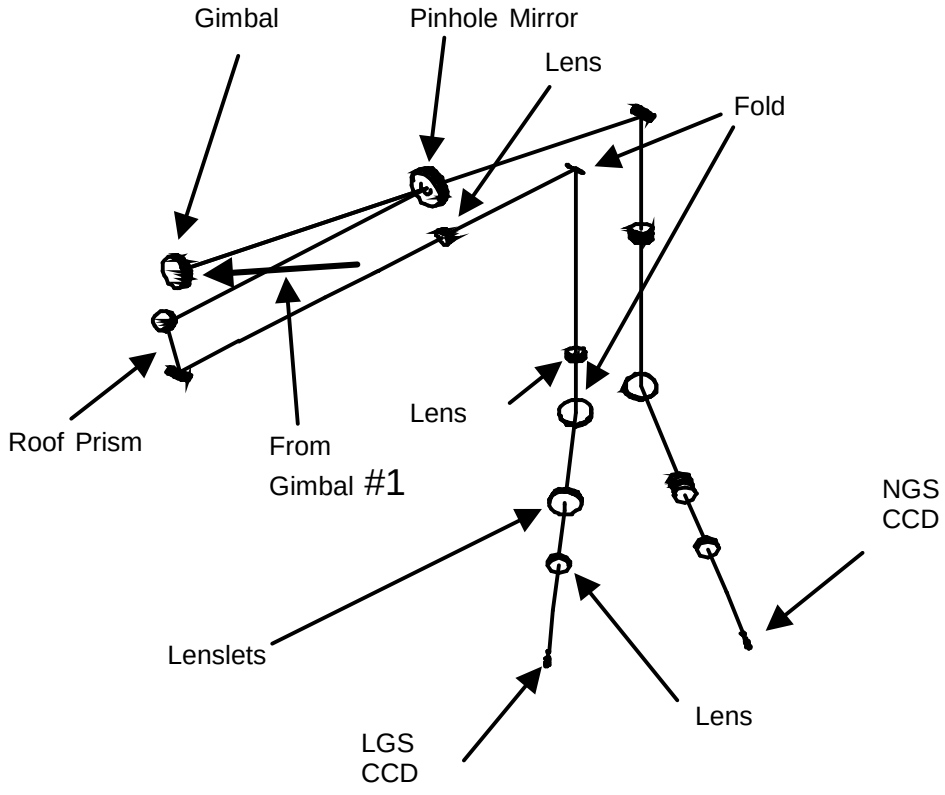

Figure 7 Laser Guide Star Optics

secondary mirror, cast by the laser beacon. Separating the two beams in this way gives higher throughput than using a dichroic beamsplitter. After this pinhole mirror, the laser beam reflects from a right-angled roof prism and returns parallel to itself. The roof prism moves axially 100 mm to refocus the laser beacon whose range distance varies with zenith distance and height of the sodium layer. Moving a roof prism uses half the travel compared with moving the CCD on a stage, and is insensitive to stage run-out in the plane of the input/output beams. Next, collimating lenses #1 and #2 each move < 5 mm axially to keep the magnification of the DM image constant on the lenslets. All of the lenses in both the laser guide-star and natural guide-star path are less than thirty millimetres in diameter. The WFS design presented here has been redone since the preliminary design review, to include reviewers' suggestions[6].

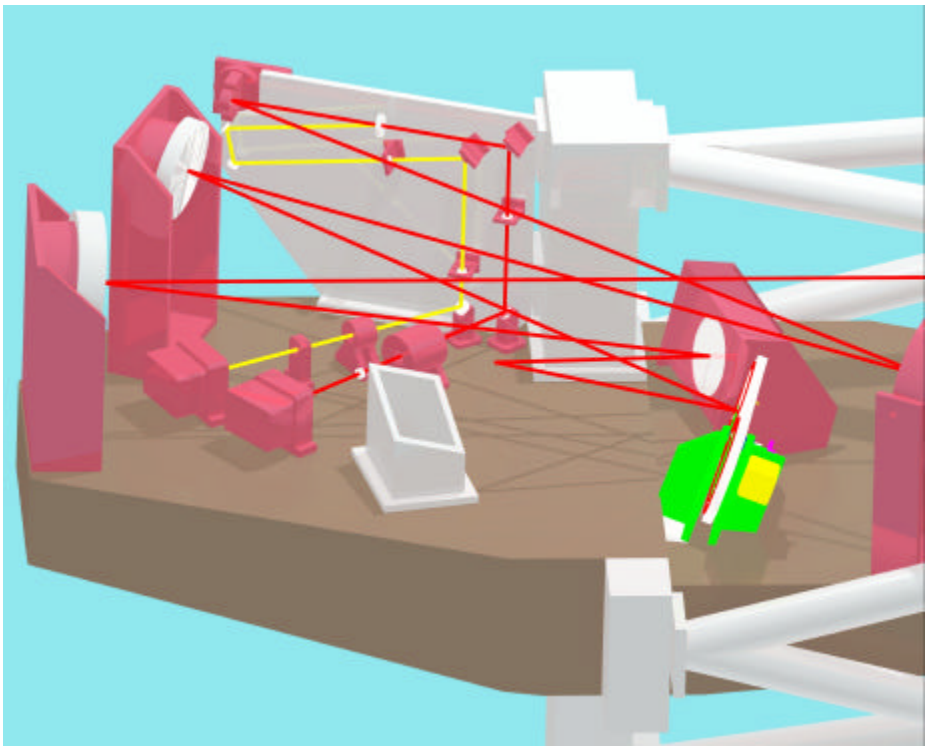

Figure 8 NGS + LGS Optics

This WFS optical arrangement with two CCDs permits cross-comparison of natural and laser beacon performance for diagnostic purposes. In figure 8, NGS + LGS Optics, you can see the natural guide starlight (dark) separated from the LGS beam (light) and detected by the two CCDs. But, Altair can only feed both WFS, if the laser launch telescope aims at a real star on-axis. This of course will not be typical during astronomical observations where the telescope will nod a few arcseconds between a series of short exposures. It is expected that the laser beacon will be re-aimed at the centre of the astronomical object of interest as it moves in the field of view.

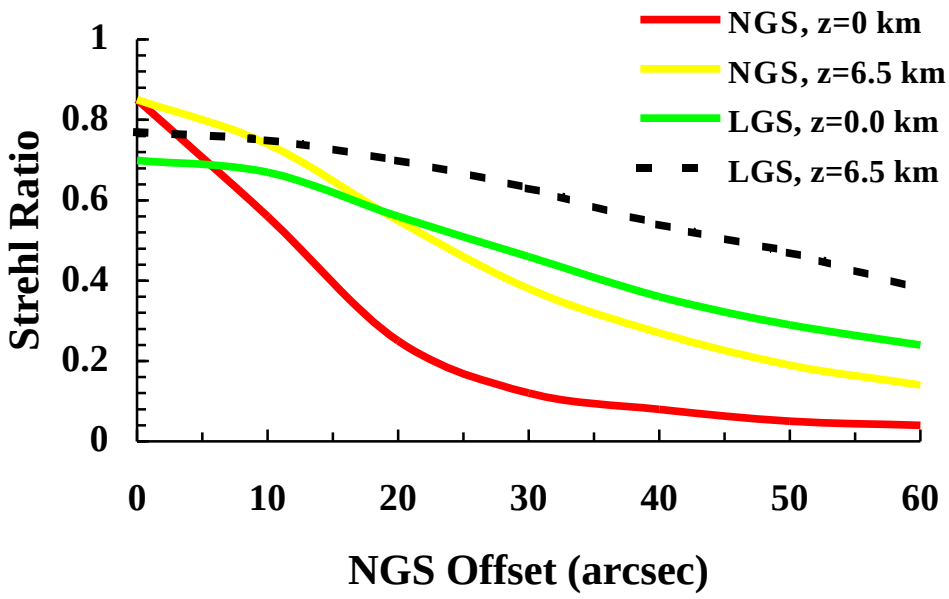

Figure 9 Strehl Reduction due to NGS offset

CONJUGATION TO ALTITUDE.

Figure 9 shows the benefit of placing the DM at an image of the layer 6.5 km in front of the telescope; it plots reduction in Strehl ratio versus the distance to a guide star. The two natural guide star curves are generally lower off-axis, and show the quality of correction versus distance from the AOWFS guide object. You can see that when the DM is conjugate to altitude, one can typically use a guide star twice as far off-axis to achieve the same image quality. This dramatically improves sky coverage, i.e., the probability of achieving a given Strehl.

The upper two laser curves are not quite the same thing. They show the reduction in Strehl, solely in the direction of the laser beacon, when Altair uses OIWFS data from a natural tip/tilt star further from the laser beacon – one cannot infer the diameter of the laser-corrected patch from this figure. Nonetheless, the graph does show that the natural tip/tilt star may be twice as far from the science object for equivalent image quality. At the same time, if you look at the left-hand end of the LGS curves, you see that conjugating the DM to altitude restores much of the loss in image quality caused by the laser-beacon cone effect.

But, conjugating to altitude does pose technical challenges that have the same root cause. Since Altair images an upper layer onto the deformable mirror, the footprint on the DM, of the guide star and the astronomical object of interest, are offset from each other. The light coming from both objects into the telescope may be thought of as cylinders angled slightly apart, but with a common base at the telescope. If we slice horizontally through both cylinders at a plane 6.5 km up, then we see two overlapping circles. The Altair collimator mirror projects these circles onto the DM.

The worst case is shown in Figure 10 for a science object on-axis and a guide star at the edge of the field of view at 1 arcminute radius. The cats-eye shaped region is the overlapping area of the DM that reflects both the guide star and astronomical object. The geometry of the guide star position determines the control matrix configuration. Which actuators are controlled by closed-loop servos, and which are extrapolated, changes with guide star location. There is a crescent of actuators on the right of the diagram that are extrapolated. Since the guide star does not illuminate this crescent region, we cannot control these actuators with servo-controllers (e.g., integrators), because there is no optical feedback of actuator position. In the face of real-world errors like roundoff and misalignment, integrators would quickly saturate. Thus our control architecture is a two-step process. After driving the illuminated actuators using modal optimization, the algorithm extrapolates the low-

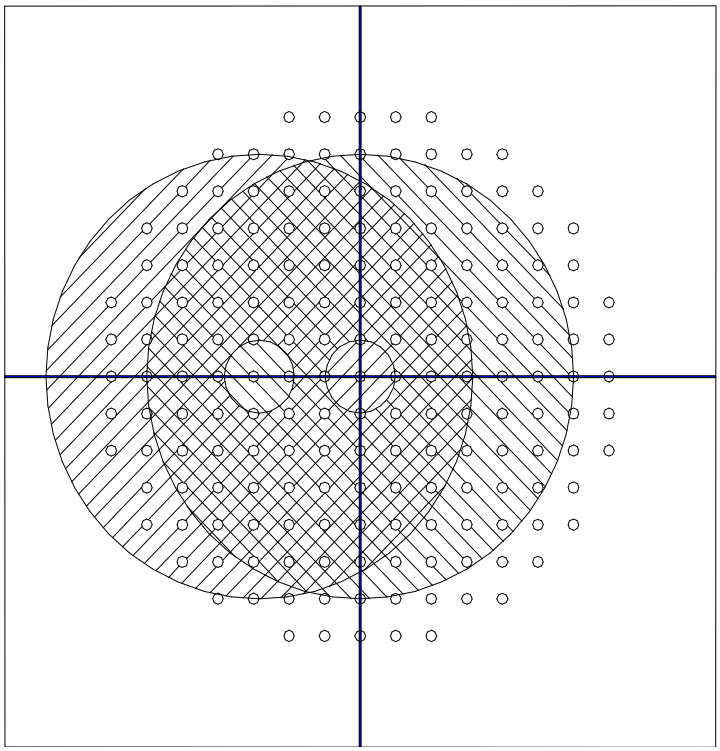

Figure 10 Worst Case off-axis guide star

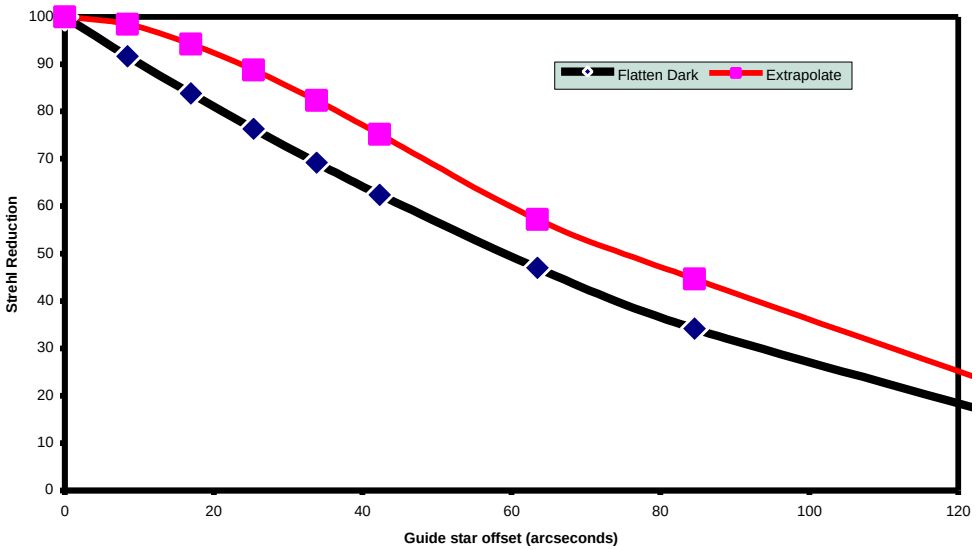

Figure 11 Extrapolation

order modes of the mirror figure, (i.e. reconstructs the drive voltages) not the WFS signals directly. Altair drives the unilluminated actuators in one step, in an open-loop scheme. This second reconstruction is required, in any event, to offload the DM quasi-static shape onto the secondary mirror and telescope control system as described below. Figure 11 shows the predicted improvement in image quality with extrapolation compared with simply flattening the 'dark' region of the DM not illuminated by the guide star.

Another complication in Altair is that for different guide star positions, the guide star illuminates different lenslets. This happens because the AOWFS optics project an image of the DM onto the lenslets, but with a field stop that admits only the guide star. Only those lenslets monitoring the guide star patch on the DM receive light. To minimize readout time, Altair continually reprograms the CCD controller to read a varying region on the CCD[3].

CONTROL SYSTEM

Altair's control system is part of the overall Gemini observatory control system. Designing Altair to work closely with the telescope has allowed us to devise nested control loops.

Figure 12, is a cartoon of the Gemini telescope and its control system, showing the Instrument Support Structure (ISS) below the primary mirror. A fold mirror diverts light into Altair where it is processed and then directed, by a central fold mirror in the ISS, to an instrument. Each instrument has a 2x2 SH WFS, (OIWFS). The AO control system processes its own AOWFS, and blends it with tip/tilt and focus signals from the OIWFS, to drive Altair's tip/tilt and deformable mirror. Altair off-loads the long-term average of its tip/tilt and focus corrections onto the secondary mirror (M2) on a fiber optic link. It also reports the first ten low-order static aberrations via Ethernet to the telescope control system (TCS), which is responsible for the primary mirror (M1) figure, for the telescope drives and for the XY collimation of the telescope.

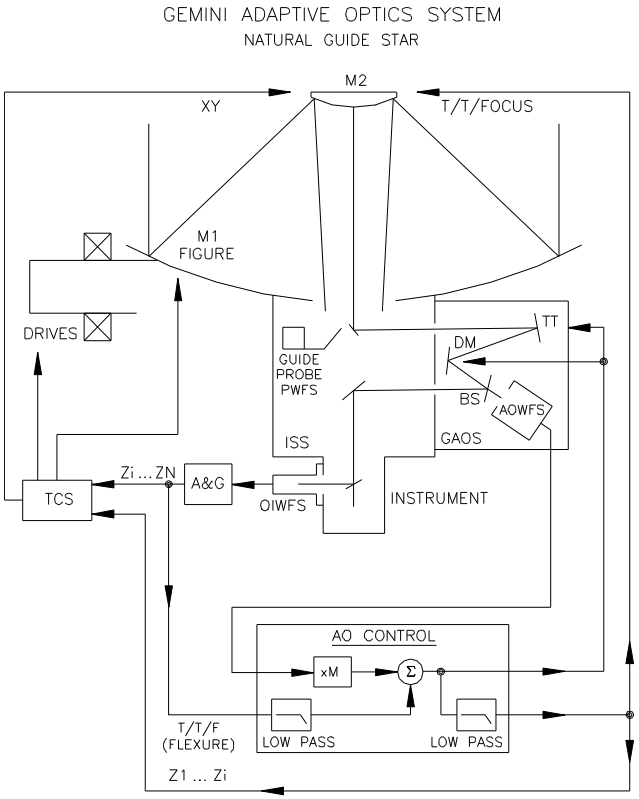

Figure 12 Control System

As mentioned, despite its varying orientation with respect to gravity, and despite being over 3 metres from focus, Altair has a structure that is not extremely stiff, because it uses the OIWFS as the reference for flexure control. The signal flow diagram

in figure 13 depicts how this works. At the top is the high-speed path from the AOWFS to the DM for the higher spatial frequencies. The low temporal frequencies of the tip/tilt and focus signals from the AOWFS reconstructor (Z2..Z4) are filtered out and replaced by measurements from the OIWFS. For laser guide stars, the OIWFS can act as a star tracker by increasing its filter bandwidth when blending it with the AOWFS.

Note, however, that Altair does not throw away the dc component of tip/tilt and focus from the AOWFS. Instead it sends them to a servo controller that slowly updates the pointing model for the two gimbal mirrors. The telescope control system tells Altair the nominal position of the guide star, and Altair steers the guide star onto the WFS. But if there is a persistent tip/tilt or focus term from the AOWFS, then this servo causes the gimbal mirrors to move and null the average seen by the AOWFS. Thus, it automatically compensates for flexure.

At the same time, the DM image is kept aligned on the lenslets by driving the centre of gravity of all the light reaching the CCD to the desired location with a low speed servo that also feeds the gimbal pointing model.

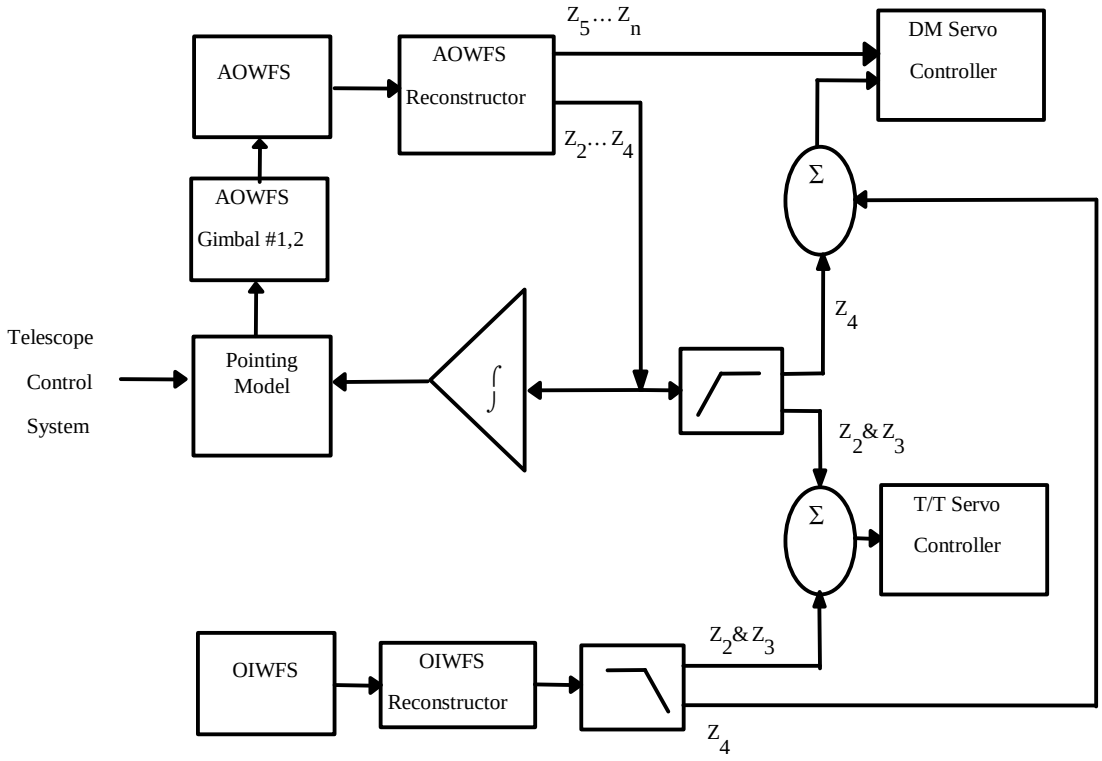

Figure 13 Blending High and Low Order WFS signals

DIFFERENTIAL OFFSET CALIBRATION AND CENTROID GAIN ESTIMATOR.

Optical differences between the AOWFS optics and the science path, mean that the best wavefront at the AOWFS, does not produce the best correction of the delivered image. Suppose that the science path had no distortions at all, but there were aberrations in the AOWFS path. When you turn the servo system on, it would copy the WFS errors onto the output beam as it nulled the measurements from the WFS. To avoid this, Altair drives the Shack-Hartmann spots to offset positions, off_{ncp} to compensate for these differential (non-common path) errors.

Altair will calibrate off_{ncp} offline with an artificial star deployed its input, together with a 20x20 SH high resolution HRWFS in the instrument support 'cube'. During calibration, the phase map will be loaded into the controller and iterated until the best image quality is delivered.

In principle, one could subtract calibrated spot positions directly from the AOWFS measured slopes; but, this creates a problem. Since the AOWFS uses 2x2 pixels per subaperture as quad cells, Shack-Hartmann spots are undersampled. Hence, measured slopes s_{meas} are contaminated by non-common path offsets off_{ncp}, scaled by a subaperture gain factor G_{sa}, which varies with seeing: $s_{meas} = (s_{atm} + off_{ncp})/ G_{sa}$ Without knowing the seeing, the scale factor G_{sa} is unknown, so the amount to subtract, off_{ncp}/ G_{sa}, is unknown. So without more information, we would spuriously introduce some of the previously calibrated non-common-path errors into the measured slopes sent to the reconstructor.

We have devised a method where Altair determines G_{sa} without requiring an external seeing monitor. The lower part of the figure, shows the high-speed signal path from the AOWFS to the DM. After the phase error reconstructor, the stored calibration phase map is subtracted, from the phase errors e, not the WFS slopes, to produce the input to the DM servo.

The servo produces mirror figure commands which are offset and scaled for each actuator individually. The DM servo tries to drive its input to null. Ideally, in equilibrium the mirror figure should match the calibration phase map. Thus the dot product of the mirror figure and the calibration phase map off_{ncp} should be unity. Deviations from unity are integrated with a long time constant (t ~ 10 s). The output of this integrator is an estimate of the correct subaperture gain. The 'Optimizer' uses this gain G_{sa}, along with other statistics gathered from the servo loop to compute a new reconstructor matrix about every ten seconds. Therefore, the 'Optimizer', as it updates the gains in the reconstructor matrix, drives the average phase error, seen by the WFS, to equal the stored calibration phase map.

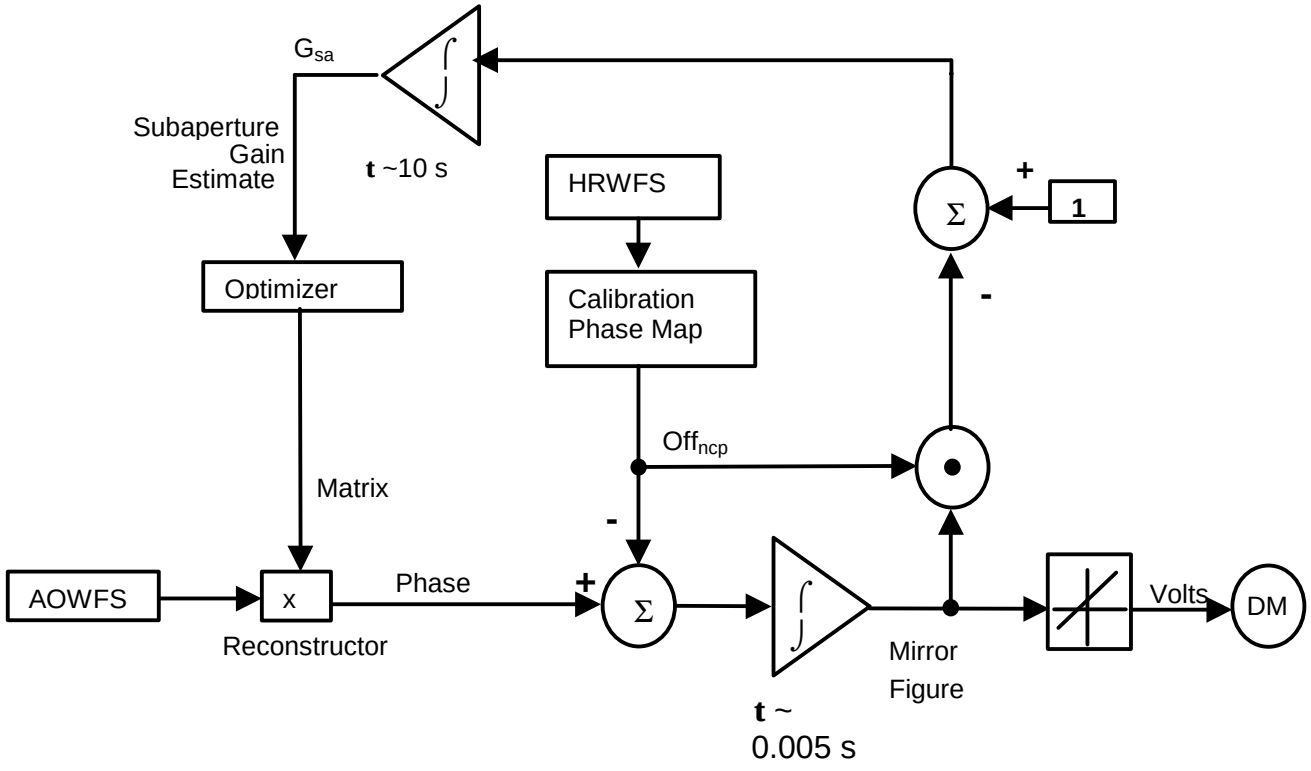

Figure 14 Centroid Gain Estimator

An analogous problem will occur with a laser beacon. Gemini plans a launch telescope behind the secondary mirror. Thus laser WFS subapertures at the edge of the pupil will see elongated spots. The spot elongation is radially symmetric, with an unvarying orientation (elongated toward the centre of the pupil). Outer subapertures have less radial gain than inner ones.

Now imagine we are guiding on a laser, and things are perfectly calibrated. The servo moves the spots to their desired positions. We deliver perfect images until for example, the sodium layer changes thickness or height. The gain of the quad cell in the radial direction will change. This unknown gain multiplies the offsets by an unknown factor. The quad cell output is again contaminated. This time, however, the subaperture gain varies radially, largely due to the sodium layer, and varies tangentially, largely as a function of seeing and the projected spot size.

By resolving the calibration phase map into radial and tangential components $off_{ncp,r}$, $off_{ncp,t}$ for each subaperture, then we can take two dot products. The tangential components will have a dot product with the mirror figure MF_t representing a common gain $G_{sa,t}$ related to seeing, for the entire pupil, and may be handled similarly to the natural guide star to derive a subaperture gain in the tangential direction. The optimizer adjusts $G_{sa,t}$ until $<MF_t \bullet G_{sa,t}> = 1$

For the radial elongation components, the subaperture gain varies linearly with radius $G_{sa,r}(r) = G_{sa,t} - k \bullet r$. The optimizer adjusts k until $<MF_r \bullet G_{sa,r}(r) > = 1$. This scheme works because we are using the natural guide star OIWFS as an absolute focus reference. Otherwise, the radial variation in subaperture gain would appear as a focus measurement.

CONCLUSION

The combination of the infrastructure provided by the Gemini North Observatory, together with the decision to conjugate the DM to 6.5 km altitude, has resulted in novel solutions to some challenging design problems for Altair, the Gemini adaptive optics system.

REFERENCES

1. "Opto-Mechanical Design of Altair, the Gemini Adaptive Optics System", Roberts, S., Singh, G. This conference.

2. "Optical Design of Altair," E. H. Richardson. This conference.

3. Design Aspects of the Reconstructor for the Gemini Adaptive Optics System (GAOS), Leslie Saddlemyer, Glen Herriot, Jean-Pierre Véran, Murray Fletcher. This conference.

4. "Laser Guide Star Provisions in Gemini Adaptive Optics System" Glen Herriot, Simon Morris, Scott Roberts, ESO workshop on LGS AO, Proceedings No. 55, June 1997

5. "Profiles of night time turbulence above Mauna Kea and isoplanatism extension in adaptive optics", René Racine & Brent Ellerbroek, SPIE 2534, 1995

6. "Wavefront Sensor Optical Design", Peter Wizinowich, Skip Radau, Keck Internal Report, 1997

7. www.hia.nrc.ca/facilities/gemini/altair/altair.html